Stability Analysis of Frictionless Grasps and Combining Frictional and Frictionless Grasps

Sushanta Kumar Saha *, Takayoshi Yamada *, Nobuharu Mimura **, and Yasuyuki Funahashi *

*: Department of Mechanical Engineering,
Nagoya Institute of Technology
Gokiso, Showa, Nagoya 466-8555, Japan
Email: sushanta, yamat@eine.mech.nitech.ac.jp

**: Department of Information Engineering,
Niigata University
Ninomachi, Igarashi, Niigata 950-2181, Japan

Abstract

This paper discusses the stability of 2D frictionless grasps and combining stability of frictional and frictionless grasps from the viewpoint of potential energy method. In many works related to the frictionless grasp, each finger is replaced by one directional virtual spring along the normal at the contact point. However, this condition is not accurate, because the frictionless condition does not mean one-spring model but means contact force condition. So, in order to represent the condition that the contact force directs to the normal at the contact point, a two-dimensional virtual spring model is essential. It is clarified that the relation between one- and two-spring cases. Some numerical examples are presented to verify our analysis. Moreover, stiffness condition of the spring for stabilization of the grasp is established. Finally, we derive stiffness matrix for both frictional and frictionless grasps from the same derivation.

***Key Words**:* stability, potential energy, frictional and frictionless grasps, stiffness condition.

1. Introduction

Human hand can easily accomplish complex and difficult tasks. So it is required for the robot hand to grasp dexterously instead of the human hand.

The fundamental ability of grasping is to maintain the grasp stable against external disturbances. In the method for analyzing the grasp stability, the robot finger is replaced by elastic finger and then stability is discussed from the viewpoint of potential energy.

If counterclockwise disturbance exerts on the grasp system as shown in Fig. 1 (a), the fingertip shifts as follows. For the frictional case, the fingertip moves to counterclockwise direction as shown in Fig.1 (b). If the frictionless case is considered, the fingertip moves to clockwise direction as shown in Fig. 1(c). So stability is greatly influenced by contact conditions.

Kaneko et al. [1] derived the stiffness matrix of frictional planar grasps by two-dimensional virtual springs, and investigated the stability. Moreover, the stiffness conditions for stabilization of the grasp were established. Mimura et al. [2] extended it to 3-dimensional grasps.

Nguyen [3] treated frictionless planar grasps. The effect of object shape at the contact to the grasp stability is also analyzed. Howard and Kumar [4] discussed the stability including the shape of the object and finger at contact points from viewpoint of restoring forces. However, the method is somewhat complex. Funahashi et al. [5] analyzed the stability from the viewpoint of potential energy using the curvatures at the contact point.

Refs. [3], [5] treated frictionless grasps by using a one-dimensional virtual spring model, where the fingertip displaced along the same line shown in Fig.1 (d). However, this condition is not accurate, because the frictionless condition does not mean one-spring model but means contact force condition. If we consider the two-dimensional displacement of the fingertip as shown in Fig. 1 (c), then it will be more significant in practical use. So the finger is replaced by a two-dimensional virtual spring and the contact force is considered along the normal at the contact. Comparing our analysis with Ref. [5], the effect of the tangential spring is considered. Stability, flexibility and energy are important factors for grasping in practical. Using the larger tangential spring stiffness, less flexibility and much energy are required to grasp the object.

Moreover, we combine the frictionless and the frictional grasps in the same derivation in section 3. The advantage of this analysis is that we need not extra calculation for each case.

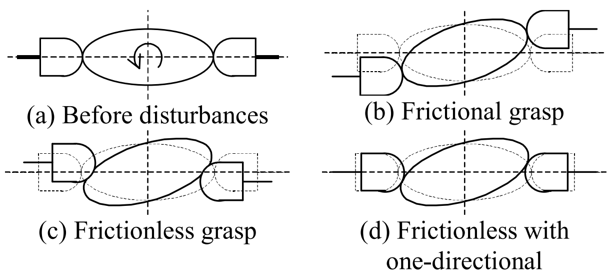

(a) Before disturbances
(b) Frictional grasp
(c) Frictionless grasp
(d) Frictionless with one-directional displacement

Fig.1: Fingertip displacements for each condition

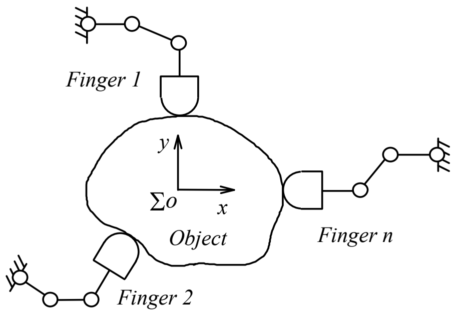

Fig.2: Object grasped by a multifingered hand

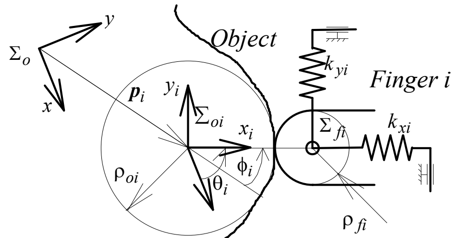

Fig.3: Coordinates and virtual springs

2. Frictionless grasp

In this section, we discuss the stability of frictionless planar grasps by a multifingered hand as shown in Fig. 2. Fig. 3 shows the i-th finger makes contact with the object.

2.1. Assumptions

For simplicity of discussions, we make the following assumptions.

(A1) 2-dimensional frictionless grasps are considered.
(A2) The shapes of the fingertip and the object are known, and the curvatures around the contact point are given.
(A3) Initial configuration is known and is in equilibrium state.
(A4) Infinitesimal object displacement is occurred.
(A5) The fingertip does not rotate.
(A6) Each finger is replaced by a two-dimensional virtual spring as shown in Fig. 3. One spring k_{xi} is along the normal and another k_{yi} is parallel to the tangent.

We define three coordinate frames shown in Fig. 3. Σ_o is an object coordinate frame. Σ_{oi} and Σ_{fi} are local coordinate frames fixed at the center of the circle of object's and finger's curvature, respectively. The *x* axes of Σ_{oi} and Σ_{fi} are along the normal. The position and the orientation of Σ_{oi} with respect to Σ_o are denoted by $\boldsymbol{p}_i$ and θ_i, respectively. The radius of curvatures for object and finger are denoted by ρ_{oi} and ρ_{fi}, respectively.

$\rho > 0$ for convex arc,
$\rho < 0$ for concave arc.

Contact point on the object with respect to Σ_o is denoted by $\boldsymbol{c}_{oi} = \boldsymbol{p}_i + [\rho_{oi}\cos\theta_i, \rho_{oi}\sin\theta_i]^T$. Initial grasping force with respect to Σ_{fi} is denoted by $[f_{xi}, f_{yi}]^T$. This force is exerted by the initial compression, $[\delta_{xoi}, \delta_{yoi}]^T$, of the i-th spring. This means

$$f_{xi} = k_{xi}\delta_{xoi},\quad f_{yi} = k_{yi}\delta_{yoi}. \tag{1}$$

From (A1), no tangential force is applied, i.e., $f_{yi} = 0$.

2.2. Relation between object and finger displacements

In this section, we derive the relationship between object and finger displacements. First, we develop the relation between Σ_{oi} and Σ_{fi} frames and then the relation between Σ_o and Σ_{oi} frames, respectively. Finally, we have the relationship between Σ_o and Σ_{fi} frames.

2.2.1 The relationship between Σ_{oi} and Σ_{fi}

We will derive the relation of Σ_{oi} and Σ_{fi}. From Fig. 4, the initial position of Σ_{fi} with respect to Σ_{oi} is

$$[\rho_{oi} + \rho_{fi}, 0]^T. \tag{2}$$

Let us denote translational and rotational displacements of contact frame Σ_{oi} as follows:

$$\varepsilon_i = [x_i, y_i, \zeta_i]^T. \tag{3}$$

Due to displacement, the position of finger shifts to

$$[x_i + (\rho_{oi} + \rho_{fi})\cos\beta_i, y_i + (\rho_{oi} + \rho_{fi})\sin\beta_i]^T. \tag{4}$$

Hence, the displacement $[\delta_{xi}, \delta_{yi}]^T$ is determined by

$$\delta_{xi} = x_i + (\rho_{oi} + \rho_{fi})\cos\beta_i - (\rho_{oi} + \rho_{fi}), \tag{5}$$

$$\delta_{yi} = y_i + (\rho_{oi} + \rho_{fi})\sin\beta_i, \tag{6}$$

where β_i is the angle between the segments. The letter β_i implies the direction of the normal.

Due to disturbances, if the finger moves $[\delta_{xi}, \delta_{yi}]^T$ with respect to Σ_{fi}, then *x* and *y* coordinates contact force are $k_{xi}(\delta_{xi} + \delta_{xoi})$ and $k_{yi}\delta_{yi}$, respectively. The

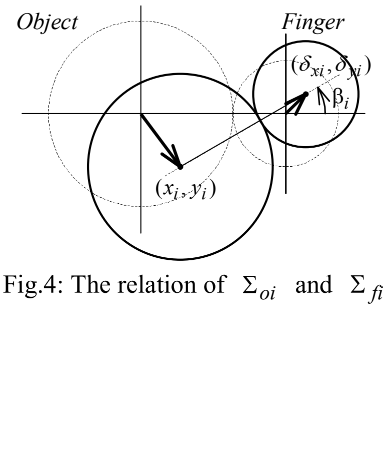

Fig.4: The relation of Σ_{oi} and Σ_{fi}

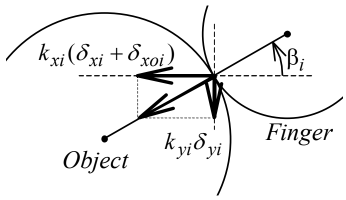

Fig.5: The relation of the contact force and the angle β_i

direction of the contact force is same to the normal as shown in Fig.5. Hence, the angle β_i is given by

$$\tan\beta_i = \frac{k_{yi}\delta_{yi}}{k_{xi}(\delta_{xi}+\delta_{xoi})}. \quad (7)$$

2.2.2. The relationship between Σ_o and Σ_{oi}

Translational and rotational displacements of the object with respect to Σ_o are denoted by x, y, and ζ, respectively. Let us define $\boldsymbol{\varepsilon}$ as

$$\boldsymbol{\varepsilon} = [x, y, \zeta]^T. \quad (8)$$

We derive the relation between Σ_o and Σ_{oi}. The displacement of Σ_{oi} is given by

$$[x_i, y_i]^T = Rot(-\theta_i)\left\{[x, y]^T + \left(Rot(\zeta) - I_2\right)\boldsymbol{p}_i\right\}, \quad (9)$$

where I_2 is a 2×2 identity matrix, $Rot(\bullet)$ is the following rotation matrix.

$$Rot(\bullet) = \begin{bmatrix} \cos(\bullet) & -\sin(\bullet) \\ \sin(\bullet) & \cos(\bullet) \end{bmatrix}. \quad (10)$$

The position vector $\boldsymbol{p}_i$ is given by

$$\boldsymbol{p}_i = p_i\left[\cos(\theta_i - \phi_i), \sin(\theta_i - \phi_i)\right]^T, \quad (11)$$

where ϕ_i is the angle between the position vector $\boldsymbol{p}_i$ and the i-th local object coordinate frame Σ_{oi}.

Then, we have

$$x_i = x\cos\theta_i + y\sin\theta_i + p_i\{\cos(\zeta - \phi_i) - \cos\phi_i\}, \quad (12)$$

$$y_i = -x\sin\theta_i + y\cos\theta_i + p_i\{\sin(\zeta - \phi_i) - \sin\phi_i\}, \quad (13)$$

$$\zeta_i = \zeta. \quad (14)$$

Substituting Eqs. (12), (13) into (5), (6) yields the relation between object displacement $\boldsymbol{\varepsilon}$ and fingertip displacement $[\delta_{xi}, \delta_{yi}]^T$.

2.3. Potential energy and stiffness matrix of the grasp

By the object displacement due to external disturbances, potential energy stored in the grasp by an n-fingered hand as shown in Fig.3 is given by

$$U(\varepsilon) = \frac{1}{2}\sum_{i=1}^{n}\{k_{xi}(\delta_{xi}+\delta_{xoi})^2 + k_{yi}\delta_{yi}{}^2\}. \quad (15)$$

Taking *Taylor* series around $\varepsilon = 0$ yields

$$U(\varepsilon) = U(0) + \varepsilon^T \nabla U\big|_{(0)} + \frac{1}{2}\varepsilon^T H \varepsilon + \cdots\cdots, \quad (16)$$

where

$$\nabla = \begin{bmatrix} \frac{\partial}{\partial x} \\ \frac{\partial}{\partial y} \\ \frac{\partial}{\partial \zeta} \end{bmatrix}, \quad H = \left.\begin{pmatrix} \frac{\partial^2 U}{\partial x^2} & \frac{\partial^2 U}{\partial x \partial y} & \frac{\partial^2 U}{\partial x \partial \zeta} \\ \frac{\partial^2 U}{\partial y \partial x} & \frac{\partial^2 U}{\partial y^2} & \frac{\partial^2 U}{\partial y \partial \zeta} \\ \frac{\partial^2 U}{\partial \zeta \partial x} & \frac{\partial^2 U}{\partial \zeta \partial y} & \frac{\partial^2 U}{\partial \zeta^2} \end{pmatrix}\right|_{(0)} = \nabla\nabla^T U\big|_{(0)}. \quad (17)$$

The initial grasp is stable if and only if the following two conditions are satisfied.

(i) $\nabla U\big|_{(0)} = 0$,

(ii) H is positive definite.

Condition (i) is satisfied by Assumption (A3). So condition (ii) is the stability condition of the grasp. The hessian H is given by

$$H = \sum_{i=1}^{n}\{k_{xi}(\nabla\delta_{xi}|_0)(\nabla\delta_{xi}|_0)^T + k_{yi}(\nabla\delta_{yi}|_0)(\nabla\delta_{yi}|_0)^T + f_{xi}(\nabla\nabla^T\delta_{xi}|_0)\}. \quad (18)$$

Hence, if $\nabla\delta_{xi}|_0$, $\nabla\delta_{yi}|_0$, $\nabla\nabla^T\delta_{xi}|_0$ are derived, then H can be determined, and the stability can be evaluated. These three terms can be derived by using Eqs. (5) and (6). Appendix A shows the detail derivation. Substituting all the values in Eq. (18), the hessian H is given by

$$H = \sum_{i=1}^{n}\left\{ k_{xi}\begin{bmatrix}\cos\theta_i \\ \sin\theta_i \\ l_{yi}\end{bmatrix}\begin{bmatrix}\cos\theta_i \\ \sin\theta_i \\ l_{yi}\end{bmatrix}^T + \frac{f_{xi}k_{yi}}{f_{xi} - k_{yi}(\rho_{oi}+\rho_{fi})}\begin{bmatrix}-\sin\theta_i \\ \cos\theta_i \\ l_{xi}-\rho_{oi}\end{bmatrix}\begin{bmatrix}-\sin\theta_i \\ \cos\theta_i \\ l_{xi}-\rho_{oi}\end{bmatrix}^T - f_{xi}\begin{bmatrix}0 & 0 & 0 \\ 0 & 0 & 0 \\ 0 & 0 & l_{xi}-\rho_{oi}\end{bmatrix}\right\}, \quad (19)$$

where

$$[l_{xi}, l_{yi}]^T := R(-\theta_i)\boldsymbol{c}_{oi} = [p_i\cos\phi_i + \rho_{oi}, p_i\sin\phi_i]^T.$$

Therefore, the stability depends on the spring stiffness, the curvatures, as well as the magnitude and position of the contact forces. If these parameters are given, then we can derive H and evaluate the stability.

The first and the third terms are the same to Ref. [5]. So we will investigate the second term of our result. In case of one-directional model, there is no translational spring in the y direction. In our case, this means $k_{yi} \to \infty$,

$$\lim_{k_{yi}\to\infty} \frac{f_{xi}k_{yi}}{f_{xi} - k_{yi}(\rho_{oi} + \rho_{fi})} = -\frac{f_{xi}}{\rho_{oi} + \rho_{fi}} .$$

Our results satisfy the one-spring model of Ref. [5].

2.4. Numerical Examples

To verify our analysis, we explore the stability conditions by using numerical examples. To simplify our analysis, objects grasped by a two-fingered hand as shown in Fig. 6. We assume that the parameters are given by

$$l_{xi} = l_x > 0,\ \ \rho_{oi} = \rho_o,\ \ \rho_{fi} = \rho_f,$$

$$f_{xi} = f_x > 0,\ \ k_{xi} = k_x > 0,\ \ k_{yi} = k_y > 0,$$

$$\theta_1 = 0,\ \ \theta_2 = \pi,\ \ \phi_i = 0.$$

Then we have

$$H = diag[k_{xx}\ \ k_{yy}\ \ k_{\zeta\zeta}],$$

where

$$k_{xx} = 2k_x,\ \ k_{yy} = \frac{2f_x k_y}{f_x - k_y(\rho_o + \rho_f)}, \tag{20}$$

$$k_{\zeta\zeta} = \frac{2f_x(l_x - \rho_o)\{-f_x + k_y(l_x + \rho_f)\}}{f_x - k_y(\rho_o + \rho_f)}. \tag{21}$$

If the total stiffness k_{xx}, k_{yy}, and $k_{\zeta\zeta}$ are positive, the

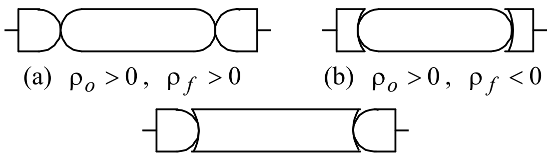

(a) $\rho_o > 0$, $\rho_f > 0$ (b) $\rho_o > 0$, $\rho_f < 0$

(c) $\rho_o < 0$, $\rho_f > 0$

Fig. 6: 2-fingered grasps

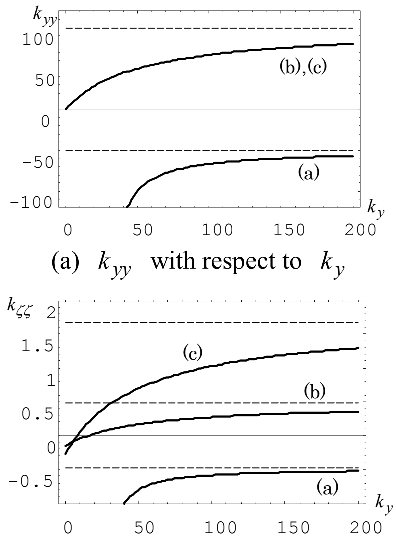

(a) k_{yy} with respect to k_y

(b) $k_{\zeta\zeta}$ with respect to k_y

Fig.7: Total stiffness vs. k_y

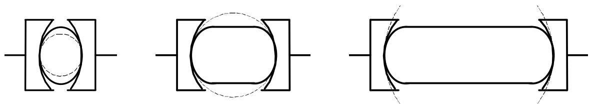

(a) case 1 (b) case 2 (c) case 3:

Fig. 8: Convex object grasped by concave fingers

grasp is stable. In Fig. 7, the solid lines depict k_{yy} and $k_{\zeta\zeta}$ with respect to k_y with $l_x = 0.1$, $f_x = 1.0$, and

(a) $\rho_o = 0.02$, $\rho_f = 0.02$,

(b) $\rho_o = 0.02$, $\rho_f = -0.04$,

(c) $\rho_o = -0.04$, $\rho_f = 0.02$.

The solid lines asymptotically join with the dotted lines (one-dimensional spring model). If k_y is enlarged, the stability is also enlarged. As a result, more energy is required to control the fingers, as well as flexibility of the grasp will be less. So it is important to derive the lowest limit of k_y.

For Fig. 6 (a), k_{yy} is always negative and the grasp is unstable. For Fig. 6(b), there are three cases shown in Fig. 8 (see Appendix B for Details). Dotted line depicts the circle with radius l_x. Case 1 ($l_x<\rho_o$) is always stable. Case 2 ($\rho_o < l_x < -\rho_f$) is unstable because object can rotate and it does not return to initial position. Case 3 ($l_x > -\rho_f$) and Fig. 6 (c) are stable if we set $k_y > f_x/(l_x + \rho_f)$. For the one-spring case, Fig. 6 (c) and Fig. 8 (c) are always stable.

2.5. Stabilization conditions for 3-finger grasps

We derive the stiffness conditions for stabilization of 3-finger grasps. In this case, contact forces intersect at one point. If the object frame Σ_o is fixed at the intersection, l_{yi} becomes zero. Eq. (19) can be rewritten as

$$H = AK_y{}'A^T + BK_xB^T - d\boldsymbol{c}\boldsymbol{c}^T,$$

where

$$K_x = diag[k_{x1}, k_{x2}, k_{x3}],\ \ K'_y = diag[k'_{y1}, k'_{y2}, k'_{y3}],$$

$$k'_{yi} = \frac{f_{xi}}{f_{xi} - k_{yi}(\rho_{oi} + \rho_{fi})} k_{yi}, \tag{22}$$

$$A = \begin{bmatrix} -\sin\theta_1 & -\sin\theta_2 & -\sin\theta_3 \\ \cos\theta_1 & \cos\theta_2 & \cos\theta_3 \\ l_{x1} - \rho_{o1} & l_{x2} - \rho_{o2} & l_{x3} - \rho_{o3} \end{bmatrix},$$

$$B = \begin{bmatrix} \cos\theta_1 & \cos\theta_2 & \cos\theta_3 \\ \sin\theta_1 & \sin\theta_2 & \sin\theta_3 \\ 0 & 0 & 0 \end{bmatrix},\ \ \boldsymbol{c} = \begin{bmatrix} 0 \\ 0 \\ 1 \end{bmatrix},$$

$$d = \sum f_{xi}(l_{xi} - \rho_{oi}).$$

If $rank(A) = 3$ is satisfied, we can define the following matrix P:

$$P = K_y{}' + \tilde{B} K_x \tilde{B}^T - d\tilde{c}\tilde{c}^T , \tag{23}$$

where $\tilde{B} := A^{-1}B$, $\tilde{c} := A^{-1}c$. Let us define Q as

$$Q = \{q_{ij}\} := d\tilde{c}\tilde{c}^T - \tilde{B} K_x \tilde{B}^T . \tag{24}$$

k'_{y1} is assigned to be

$$k'_{y1} > q_{11} . \tag{25}$$

k'_{y2} is assigned to be

$$k'_{y2} > \frac{q_{12}{}^2}{k'_{y1} - q_{11}} + q_{22} . \tag{26}$$

Finally, k'_{y3} is assigned to be

$$k'_{y3} > \frac{q_{23}{}^2 (k'_{y1} - q_{11}) + q_{13}{}^2 (k'_{y2} - q_{22}) + 2q_{12}q_{13}q_{23}}{(k'_{y1} - q_{11})(k'_{y2} - q_{22}) - q_{12}{}^2} + q_{33} , \tag{27}$$

then the grasp is made stable. From Eqs. (22) and (25), k_{y1} must satisfy the following condition

$$\frac{f_{x1}k_{y1}}{f_{x1} - k_{y1}(\rho_{o1} + \rho_{f1})} > q_{11} .$$

In the similar way, we have the conditions of k_{y2} , k_{y3} from Eqs. (22), (26) and (27).

3. Combining frictional and frictionless grasps

In the previous section, we have analyzed the frictionless grasps. Many authors have investigated the frictional and the frictionless cases separately. But there has been no previous work on the grasp stability by a multifingered hand with combining frictional and frictionless grasps. Fig. 9 depicts that the i-th finger makes contact with the object for frictional and frictionless cases.

If the object moves to upward direction and rotates to counterclockwise direction, for the frictional case, the finger rotates to the upward direction. The position of the finger is given by

$$\alpha_i = \rho_{oi}\zeta_i / (\rho_{oi} + \rho_{fi}) .$$

In the frictionless case, the finger slips to downward direction. The position of the finger is given by β_i of Eq. (7).

In this section, we combine the frictional and the frictionless grasps by incorporating a new parameter λ . $\lambda = 1$ for frictional case and $\lambda = 0$ for frictionless case. Combining the above two conditions yields

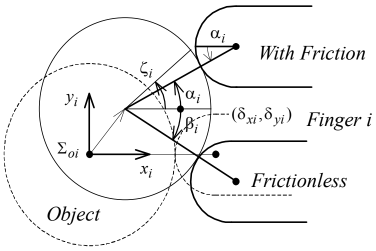

Fig.9: Frictional and frictionless grasps.

$$\gamma_i = \lambda\alpha_i + (1 - \lambda)\beta_i . \tag{28}$$

From Fig.9, the compression of the spring is given by

$$\delta_{xi} = x_i + (\rho_{oi} + \rho_{fi})\cos\gamma_i - (\rho_{oi} + \rho_{fi}) ,$$

$$\delta_{yi} = y_i + (\rho_{oi} + \rho_{fi})\sin\gamma_i . \tag{29}$$

By using Appendix C, the hessian becomes

$$H = \sum_{i=1}^{n} \left\{ k_{xi} \begin{bmatrix} \cos\theta_i \\ \sin\theta_i \\ l_{yi} \end{bmatrix} \begin{bmatrix} \cos\theta_i \\ \sin\theta_i \\ l_{yi} \end{bmatrix}^T \right.$$

$$+ \frac{k_{yi}(f_{xi} - \lambda^2 F_i)}{(f_{xi} - F_i)} \times \begin{bmatrix} -\sin\theta_i \\ \cos\theta_i \\ l_{xi} - \rho_{oi} \end{bmatrix} \begin{bmatrix} -\sin\theta_i \\ \cos\theta_i \\ l_{xi} - \rho_{oi} \end{bmatrix}^T$$

$$+ \lambda^2 \rho_{oi} k_{yi} \{ \begin{bmatrix} 0 \\ 0 \\ 1 \end{bmatrix} \begin{bmatrix} -\sin\theta_i \\ \cos\theta_i \\ l_{xi} - \rho_{oi} \end{bmatrix}^T + \begin{bmatrix} -\sin\theta_i \\ \cos\theta_i \\ l_{xi} - \rho_{oi} \end{bmatrix} \begin{bmatrix} 0 \\ 0 \\ 1 \end{bmatrix}^T \}$$

$$\left. - \{ \frac{(\lambda\rho_{oi})^2 (f_{xi} - F_i)}{(\rho_{oi} + \rho_{fi})} + f_{xi}(l_{xi} - \rho_{oi}) \} \begin{bmatrix} 0 \\ 0 \\ 1 \end{bmatrix} \begin{bmatrix} 0 \\ 0 \\ 1 \end{bmatrix}^T \right\} , \tag{30}$$

where $F_i := k_{yi}(\rho_{oi} + \rho_{fi})$. The above stiffness matrix is the combination of the frictional and the frictionless grasps. If we substitute $\lambda = 1$, then our result is same to the frictional case of Ref. [5]. On the other hand, if we substitute $\lambda = 0$, then Eq. (30) becomes Eq. (19).

4. Conclusions

In order to consider contact force conditions, we have introduced the frictionless two-dimensional virtual spring model. And the stiffness matrix for the frictionless planar grasp has been established. Then we have the following results.

(i) If tangential spring k_y tends to ∞ , then our two-dimensional model becomes the one-dimensional model and our result satisfies the result of Ref. [5].

(ii) The stability is proportional to k_y .

If k_y is assigned to be a large value, much energy is required to control the fingers.

(iii) We have also derived the lowest limit of k_y to stabilize the grasps.

(iv) Moreover we have unified the frictional and the frictionless cases with incorporating the parameter λ. Its value is 1 and 0 respectively for the above cases.

The advantage of combining two kinds of grasp is that we need not separate calculation for each case. Finally, it is shown that the stability depends on the spring stiffness, object and finger curvatures, as well as contact position and forces.

Acknowledgments

Authors would like to thank Mr. T. Mouri and Mr. Y. Katayama of our Lab. for their useful comments.

References

[1] M. Kaneko, N. Imamura, K. Yokoi, and T. Tanie, Stiffness model based grasp stability analysis of multifingered hand with friction, Journal of Rob. Society, Japan, Vol.7, No.3, pp.161-171, 1989 (In Japanese).

[2] N. Mimura and Y. Funahashi, Grasp stability analysis of three fingered hand in three dimensions, Trans. Jpn. Soc. Mech. Eng., Vol. 57, No. 537, Series C, pp. 1631-1638, 1991 (In Japanese)

[3] V. D. Nguyen, Constructing Stable Grasp, Int. J. of Robotics Research, Vol.8, No.1, Feb, 1989, pp.26-37

[4] W. H. Howard and V. Kumar, Stability of Planar Grasp, Proc. 1994 IEEE Int. Conf. on Robotics and Automation, 1994, pp.2822-2827

[5] Y. Funahashi, T. Yamada, M. Tate, and Y. Suzuki, Grasp Stability Analysis Considering the Curvatures at Contact Point, Proc. IEEE Conf. Robotics and Automation, pp. 3040-3046, 1996.

Appendix A

The 1st and the 2nd order derivatives of Eqs. (5) and (6) at initial condition are given by

$$\nabla \delta_{xi}\big|_0 = \nabla x_i\big|_0 ,$$

$$\nabla \delta_{yi}\big|_0 = \nabla y_i\big|_0 + (\rho_{oi} + \rho_{fi})(\nabla \beta_i\big|_0),$$

$$\nabla\nabla^T \delta_{xi}\big|_0 = \nabla\nabla^T x_i\big|_0 - (\rho_{oi} + \rho_{fi})(\nabla \beta_i\big|_0)(\nabla \beta_i\big|_0)^T ,$$

where $\nabla x_i\big|_0$, $\nabla y_i\big|_0$, $\nabla\nabla^T x_i\big|_0$ are given by

$$\nabla x_i\big|_0 = [\cos\theta_i, \sin\theta_i, p_i \sin\phi_i]^T ,$$

$$\nabla y_i\big|_0 = [-\sin\theta_i, \cos\theta_i, p_i \cos\phi_i]^T ,$$

$$\nabla\nabla^T x_i\big|_0 = \begin{bmatrix} 0 & 0 & 0 \\ 0 & 0 & 0 \\ 0 & 0 & -p_i \cos\phi_i \end{bmatrix}.$$

Taking the 1st derivative of Eq. (7), we have

$$k_{xi}(\delta_{xi} + \delta_{xoi})\frac{1}{\cos^2 \beta_i}\nabla\beta_i + k_{xi}(\tan\beta_i)\nabla\delta_{xi} = k_{yi}\nabla\delta_{yi}$$

If we consider the initial conditions, then we have

$$\nabla\beta_i\big|_0 = \frac{k_{yi}}{f_{xi} - k_{yi}(\rho_{oi} + \rho_{fi})}\nabla y_i\big|_0 . \qquad (31)$$

Appendix B

For Fig. 6 (a), it is shown in Fig. 4 that y_i and β_i always move to opposite direction due to two convex curves. So $\{f_x - k_y(\rho_o + \rho_f)\}$ is negative.

For Fig. 6 (b), k_{yy} is. positive because $(\rho_o + \rho_f) < 0$ and $\{f_x - k_y(\rho_o + \rho_f)\} > 0$. Now we investigate the conditions which make $k_{\zeta\zeta}$ positive. From Eq. (21), we have following two conditions:

(i) if $(l_x + \rho_f) < 0$, $(l_x - \rho_o)(k_y - \frac{f_x}{l_x + \rho_f}) < 0$,

(ii) if $(l_x + \rho_f) > 0$, $(l_x - \rho_o)(k_y - \frac{f_x}{l_x + \rho_f}) > 0$.

From (i) and (ii), we have the following 4 cases shown in Table 1. Physically, k_y is always positive. For case 1, $f_x/(l_x + \rho_f) < 0$, $k_{\zeta\zeta}$ is positive for any $k_y > 0$. For case 2, k_y has no positive value. Case 3, if $0 < k_y < f_x/(l_x + \rho_f)$, then the grasp is unstable. Case 4, $-\rho_f < l_x < \rho_o$ is practically impossible.

Table 1: Stabilization conditions

Case	$l_x : \rho_f$	$l_x : \rho_o$	Condition for k_y	
1	$l_x < -\rho_f$	$l_x < \rho_o$	$k_y > f_x/(l_x + \rho_f)$	stable
2	$l_x < -\rho_f$	$l_x > \rho_o$	$k_y < f_x/(l_x + \rho_f)$	unstable
3	$l_x > -\rho_f$	$l_x > \rho_o$	$k_y > f_x/(l_x + \rho_f)$	conditionally stable
4	$l_x > -\rho_f$	$l_x < \rho_o$	$k_y < f_x/(l_x + \rho_f)$	unrealistic

Appendix C

From Eq. (29), we have

$$\nabla\delta_{xi}\big|_0 = \nabla x_i\big|_0 , \quad \nabla\delta_{yi}\big|_0 = \nabla y_i\big|_0 + (\rho_{oi} + \rho_{fi})(\nabla\gamma_i\big|_0),$$

$$\nabla\nabla^T\delta_{xi}\big|_0 = \nabla\nabla^T x_i\big|_0 - (\rho_{oi} + \rho_{fi})(\nabla\gamma_i\big|_0)(\nabla\gamma_i\big|_0)^T .$$

From Eq. (28), we have

$$\nabla\gamma_i = \lambda(\nabla\alpha_i) + (1-\lambda)(\nabla\beta_i),$$

$$\nabla\nabla^T\gamma_i = \lambda(\nabla\nabla^T\alpha_i) + (1-\lambda)(\nabla\nabla^T\beta_i),$$

$$\nabla\alpha_i\big|_0 = \frac{\rho_{oi}}{\rho_{oi} + \rho_{fi}}[0\ \ 0\ \ 1]^T .$$